Lithuanian Journal of Physics, Vol. **51**, No. 3, pp. 212–220 (2011)

^{1}H and ^{13}C NMR STUDY OF PHASE TRANSITION AND MOLECULAR MOTION IN IONIC LIQUIDS FORMING LYOTROPIC LIQUID-CRYSTALLINE IONOGELS

V. Balevičius, L. Džiaugys, F. Kuliešius, and A. Maršalka

Faculty of Physics, Vilnius University, Saulėtekio 9, LT-10222 Vilnius, Lithuania
E-mail: vytautas.balevicius@ff.vu.lt

Received 8 June 2011; revised 21 September 2011; accepted 21 September 2011

The room temperature ionic liquid (RTIL) 1-decyl-3-methyl-imidazolium bromide [C_{10}mim][Br], dissolved in water, was studied using ^{1}H and ^{13}C NMR spectroscopy. The manifestation of phase transitions and fine features of molecular motion in NMR spectra upon changing temperature and composition have been analysed. The ^{1}H NMR line shape typical for anisotropic fluids with zero biaxiality (asymmetry) of magnetic shielding and the chemical shift anisotropy (CSA) of *ca* 0.33 ppm was observed and attributed to water molecules. CSA values for ^{13}C nuclei have been found in the range of 1.2–1.7 ppm. The difference between lyotropic liquid-crystalline (LC) ionogel phase and the solid one has been revealed, where the motions of RTIL and water molecules have been found to be dynamically segregated. The anisotropic ^{13}C NMR signal shape at 16.89 ppm shows the difference between LC ionogel and the lamellar phases, where usually the decreasing order parameter moving along hydrocarbon chain from the polar head is observed. It indicates, that the terminal $-CH_3$ groups are more ordered and the supramolecular structures of [C_{10}mim][Br], similar to some higher micellar RTIL aggregates are expected. In order to explain the experimental observations, the quantum chemistry DFT calculations of ^{1}H and ^{13}C magnetic shielding tensors of [C_{10}mim][Br] and various H-bond structures of H_2O were performed.

Keywords: properties of molecules and molecular ions, line and bands widths, shapes and shifts, NMR and relaxation

PACS: 33.15.-e, 33.70.Jg, 76.60.-k, 64.75.+g, 82.60.-s

1. Introduction

Technological developments of so called 'smart' materials are continuously boosting over the whole past decade [1–7]. Materials are classified as 'smart' if they possess an intrinsic ability to sense and definitely to respond to various external stimuli in a predictable way ([2] and references therein). The research of these features open new technological vista for various sensors, molecular machines, switches, controllers, etc. Ionic liquids (ILs), or sometimes specifying more precisely – room temperature ionic liquids (RTILs), which, according to definition, are compounds consisting entirely of ions, but in contrast to 'traditional' salts they are liquids already at, or close to, room temperature [8, 9], are widely and successfully applied creating multifunctional materials and compositions [3–7]. Selecting combinations of anionic and cationic subsystems one can alter defined physical and chemical properties of RTILs getting possibilities to sense and to control various molecular processes in these media. In many of their applications RTILs are employed as co-solvents in composition together with other substances that can vary the properties of the systems very significantly, supplying them many appealing features. Moreover, these systems get into the class of so-called 'complex fluids.' The defining feature of a complex fluid is the presence of mesoscopic length scale that plays a key role for the properties of the system [10]. All these make RTILs very attractive not only for technologies, but for research as well.

Gels, an important class of soft matter, have attracted considerable attention in areas of biomaterials, electrooptics, and as templates for the preparation of mesoporous materials and ordered thin films [3]. In certain cases some gels and ionogels can be considered behaving as 'smart' materials. Recently it was demonstrated that a lyotropic liquid-crystalline gel can be formed at certain conditions by interactions between long chain imidazolium-based RTILs and water [3, 4]. The purpose of present work was to study the temperature and composition effects on the phase transitions and molecular motion of one of imidazolium-based room-temperature ionic liquid, namely, the 1-decyl-3-methyl-

 ISSN 1648-8504

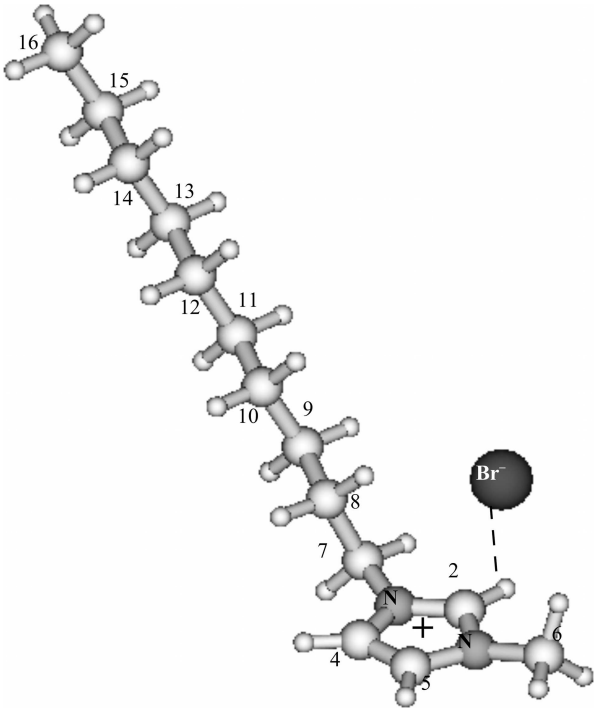

Fig. 1. Molecular structure of [C_{10}mim][Br] predicted by DFT calculation (full optimization using B3LYP/6-31++G**, *in vacuo*).

imidazolium bromide ([C_{10}mim][Br]) in aqueous solutions applying ^{1}H and ^{13}C NMR spectroscopy. In order to obtain additional insight into the experimental observations, the quantum chemistry DFT calculations of the electronic structure and the ^{1}H and ^{13}C magnetic shielding tensors of [C_{10}mim][Br] and various H-bond structures of H_2O were performed.

2. Experiment

The 1-decyl-3-methyl-imidazolium bromide ([C_{10}mim][Br], from Merck KGaA, Darmstadt) was dried under vacuum at 80 °C for one day. Its structure and atom numbering are shown in Fig. 1. The water used was freshly bidistilled. The samples containing [C_{10}mim][Br] in water solution were prepared by weighing ($\pm$0.1 mg) the components.

NMR experiments were carried out on a Bruker *Avance II 400* NMR spectrometer operating at 400 and 100 MHz for ^{1}H and ^{13}C respectively using 5 mm BBO probe-head. The temperature in a probe over the range of 288–368 K was controlled with an accuracy of $\pm$0.5 K. The signal of 4,4-dimethyl-4-silapentane-1-sulfonic acid (DSS) in D_2O solution in capillary insert was used as the reference and then converted in δ-scale respect tetramethylsilane (TMS) taking $\delta(\mathrm{DSS}) = 0.015$ ppm [11]. The D_2O in the same capillary insert was used for locking.

3. DFT calculations

The calculations of the magnetic shielding tensors of 1-decyl-3-metil- imidazolium bromide [C_{10}mim][Br] and various H-bond structures of H_2O have been performed using the density functional theory (DFT). The applied approach was checked in various cases earlier [12–14] and found to be adequate for this purpose.

The full geometry optimization in the ground state was performed *in vacuo* using the B3LYP functional combined with the 6-31++G** basis set (Fig. 1). The magnetic shielding tensors ($\boldsymbol{\sigma}$) have been calculated also *in vacuo* applying the modified hybrid functional of Perdew, Burke, and Ernzerhof (PBE1PBE) with the 6-311++G(2d, 2p) basis set. Gaussian 03 program [15] was used for all our calculations. The gauge-including atomic orbital (GIAO) approach [16] was used to ensure gauge invariance of the results.

The principal components of the ^{1}H and ^{13}C chemical shift tensors (δ_{ij}, $i,j = X,Y,Z$) were obtained subtracting those of $\boldsymbol{\sigma}$ from the isotropic part of magnetic shielding tensor of TMS ($\boldsymbol{\sigma}^{\mathrm{iso}}(\mathrm{TMS})$ values for ^{1}H and ^{13}C nuclei were taken from [17]), i. e. $\boldsymbol{\delta} = \mathbf{1}\,\boldsymbol{\sigma}^{\mathrm{iso}}(\mathrm{TMS}) - \boldsymbol{\sigma}$ and used to construct other parameters of magnetic shielding. These parameters, namely,

isotropic chemical shift:

$$\delta^{\mathrm{iso}} = \frac{1}{3}(\delta_{XX} + \delta_{YY} + \delta_{ZZ})\,,$$

chemical shift anisotropy (CSA):

$$\delta^{\mathrm{aniso}} = \delta_{ZZ} - \delta^{\mathrm{iso}}\,, \qquad (1)$$

biaxiality (asymmetry):

$$\eta = \frac{\delta_{YY} - \delta_{XX}}{\delta^{\mathrm{aniso}}}\,,$$

are directly related to the NMR signal shape ([18] and Fig. 2) and thus are more useful when analysing the measured spectra for practical aspects.

4. Results and discussion

It is known from prior studies that some of imidazolium-based RTILs [$C_n$mim][X] with sufficiently long alkyl chains (n = 12–18) can form in the neat compound and in aqueous solution various liquid crystalline (LC) phases [3, 4, 19]. For those with shorter alkyl chains (n = 2–10) an isotropic liquid phase was deduced at room temperature [3]. This is only partially

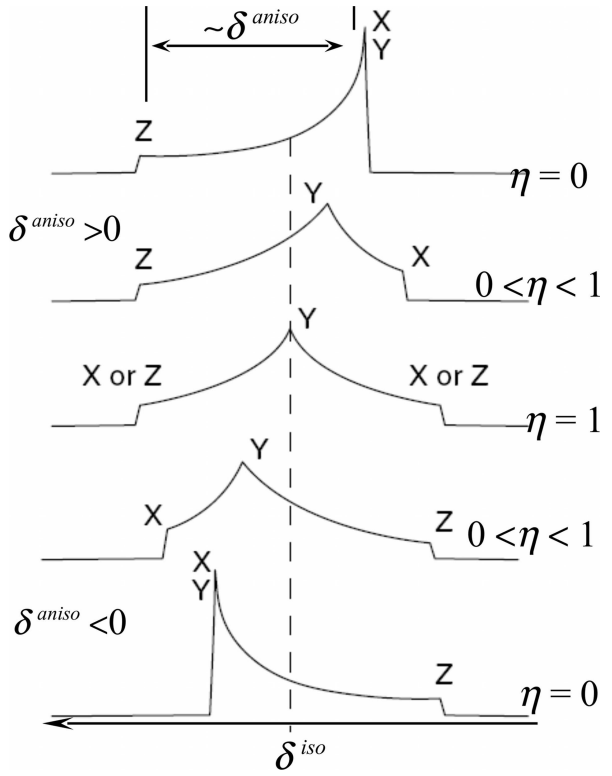

Fig. 2. NMR signal shape dependences on the anisotropic properties of magnetic shielding parameters δ^{aniso} (chemical shift anisotropy) and η (asymmetry).

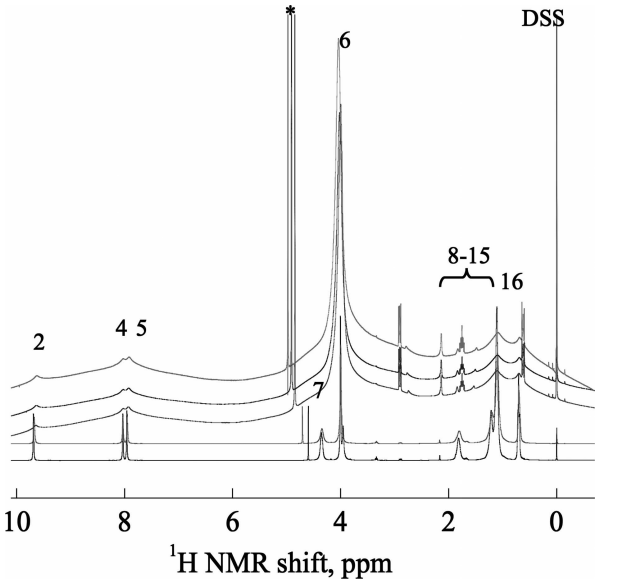

Fig. 3. ^{1}H NMR of spectra of [C_{10}mim][Br]/water solution (5% w/w of H_2O) in the solid (T = 278, 283, 288 K, from up to down, respectively) and liquid (at 300 and 310 K) phases; $*$ marks the HDO signal from the D_2O/DSS capillary insert; for the signal numbering see Fig. 1.

true. As it follows from ^{1}H, ^{13}C, and ^{81}Br NMR spectra of [C_{10}mim][Br] that have been analysed [20, 21] studying the mesoscopic effects, only the cationic subsystem, i. e. $C_{10}mim^+$, in the neat RTIL, indeed behaves as being in the isotropic liquid phase. The shape of ^{1}H and ^{13}C NMR peaks in the neat [C_{10}mim][Br] at room temperature was found to be perfectly Lorentzian, while the complex contour of ^{81}Br NMR signal, typical for anisotropic liquid, was registered. Also note that the complex shaped NMR signal of $^+$C–H...Br$^-$ proton has been registered in the very initial stage, when [C_{10}mim][Br] was just mixed with water [22]. This signal changes (within minutes) to Voigt profile with Gauss contribution as dominant and later on starts slowly to evolve towards Lorentz-shaped contour. This observation was attributed to the appearance of long-lived nonequilibrium aggregates and microheterogeneities in [C_{10}mim][Br]/water solution [22].

Addition of water to [C_{10}mim][Br] causes its conversion from a viscous liquid to a gel possesing the optical birefringence [3]. It was identified as LC ionogel. This gel was found to be stable over ∼5–40% w/w range [3]. For [C_{12}mim][Br] the LC phases were determined more precisely being lamellar (L_α) and hexagonal (H_1 ones [4]. Moreover, depending on the temperature and the composition, the regions of various coexisting phases (solid, LC, and liquid ones among them) may appear on the phase diagram [4].

The samples containing 5 and 15% w/w of H_2O, i. e. those at the onset and close to the middle of the composition range, where LC ionogel phase was certainly stated by means of the polarized optical micrography [3], have been prepared and their ^{1}H and ^{13}C NMR spectra investigated. Some selected ^{1}H NMR spectra around the phase transition point are shown in Fig. 3. The main peak positions in spectra are comparable with those for [C_8mim][Cl] and [C_{12}mim][Br] given respectively in [23, 24]. The spectra registered at room temperature consist of narrow and symmetrical in shape peaks that are common for the isotropic liquids. Thus [C_{10}mim][Br]/water mixture with the lower content of water exhibits at room temperature a typical isotropic liquid phase behaviour.

However, a remarkable feature of this system is a very weak dependence of the chemical shift of H2 proton on temperature ($\Delta\delta/\Delta T \sim +10^{-3}$ ppm/deg, Fig. 4) in comparison with that for H_2O (in solution) or HDO (in D_2O capillary insert) signals ($\Delta\delta/\Delta T \sim -10^{-2}$ ppm/deg) [25]. Moreover, the slopes $\Delta\delta/\Delta T$ even have opposite signs. It reveals that the Br$^-$...H–C2$^+$ bridge in [C_{10}mim][Br] behaves quite differently from the 'traditional' H-bonds. These observations can somehow correlate with the results of FTIR studies on the other imidazolium-based ILs, where the C2–H and

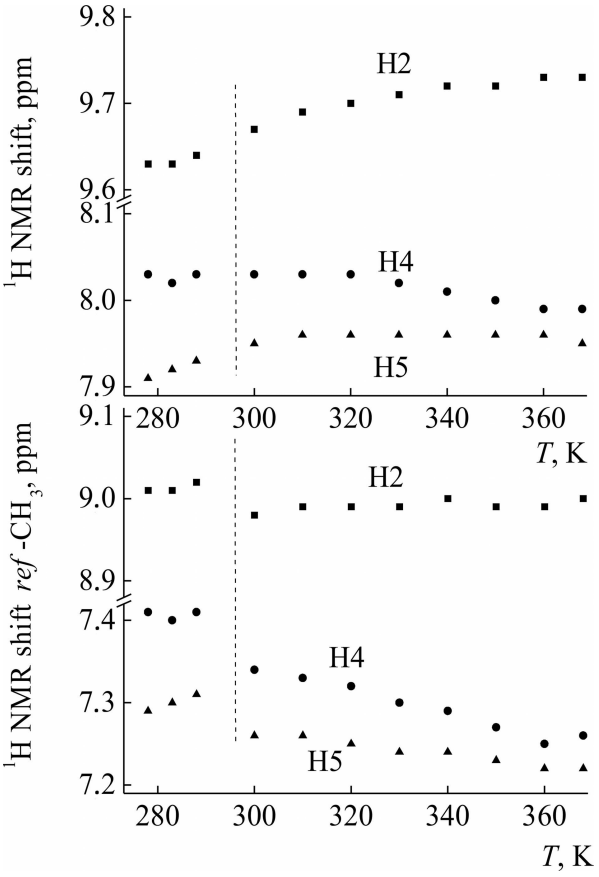

Fig. 4. ^{1}H NMR shift dependences on temperature with respect to the external DSS signal (the upper graph) and with respect to the terminal $-C(16)H_3$ group protons (i. e. the 'internal' standard; the lower graph). More comments in text.

C4,5–H stretching bands yielding a drastic blue-shift at increasing dilution in water have been found [26]. Also note the mutual convergence of H4 and H5 signals in ^{1}H NMR spectra at increasing temperature (Fig. 4), similarly to that observed at the dilution of $[C_{10}mim][Br]$ in media of increasing polarity [25]. It could have happened that the bromine anion was pushed by the intensified thermal motion from the equilibrium position of $[C_{10}mim][Br]$ (Fig. 1) closer to the vertical mirror plane of the imidazolium ring. This would make the positions 4 and 5 more equivalent and thus cause the mutual convergence of H4 and H5 signals.

The phase transition in the sample of this composition (5% w/w of H_2O) occurs at the cooling at *ca* 295 K (Figs. 3 and 4). Instead of narrow symmetric peaks the broad more or less asymmetrically shaped signals are seen in ^{1}H NMR spectra (Fig. 3) that are common for lyotropic LC phases [27]. The degree of asymmetry of the signal contours indicates that the biaxiality of this phase should be rather close to 1 (see the shapes in Fig. 2). On the other hand, the changes and high distortion in relative intensities of the peaks points to the heterogeneity of this phase. It should be discussed in more detail. Comparing the drastic drop in the signal heights with those of DSS and HDO from the capillary insert below the phase transition temperature (Fig. 3), it becomes clear that some part of protons in the sample do not longer contribute the high resolution NMR signals. It means their motion gets frozen in this phase. This is in a good agreement with the phase diagram of $[C_{12}mim][Br]/H_2O$ data [4] that the solid, lamellar (L_α), or hexagonal (H_1) phases can coexist at low content of water. Furthermore, very intensive signal at $\sim$4 ppm composed of the overlapped ^{1}H NMR signals of H6, H7, and water protons is observed (Fig. 3). According to the molecular structure of $[C_{10}mim][Br]$ and the fact that the composition of 5% w/w of H_2O sample corresponds to 0.6 mole fraction of RTIL and 0.4 mole fraction of water, the integral intensity of those signals should be only 2–6 times higher than for H2, H4, H5, or H16 and almost one order lower than for H8. . .H15 protons in the hydrocarbon chain (signal group at 0–2 ppm, Fig. 3). The opposite was observed in reality. This unusually intensive peak can be attributed to the signal of H_2O molecules averaged over various water H-bond states and sites around RTIL. Some of them were identified in Raman spectra using principal components and 2D correlation analysis [21]. It means that the mobility of water molecules in the lyotropic phase survives and is intensive and high enough whereas the dynamics of most RTIL units is significantly restricted or even frozen.

Note that this phase transition is stronger pronounced, namely, the discontinuous changes are much clearly seen on the temperature dependences of the 'internal' chemical shifts of imidazolium ring protons, i. e. the chemical shifts with respect to the signal of terminal $-CH_3$ group (Fig. 4). While referring to the 'external' DSS signal (Sec. 2), the changes in the macroscopic parameters (e. g. bulk magnetic susceptibility) can affect the resonances of both the sample and the insert capillary significantly. In consequence, rather fine effects of this phase transition on the 'external' chemical shifts are faded.

At the higher content of water ($\sim$15% w/w of H_2O) the sample converts into a stable gel, which resists flow upon gravity, already at room temperature. New signals appear in ^{1}H and ^{13}C NMR spectra (Figs. 5 and 6) that are absent in isotropic liquid phase. The shapes of these signals are typical for anisotropic liquids, however, with the biaxiality close to zero (Fig. 2). Thus they differ from the case above of 5% w/w of H_2O in the mixture (Fig. 3). The experimental NMR contours were

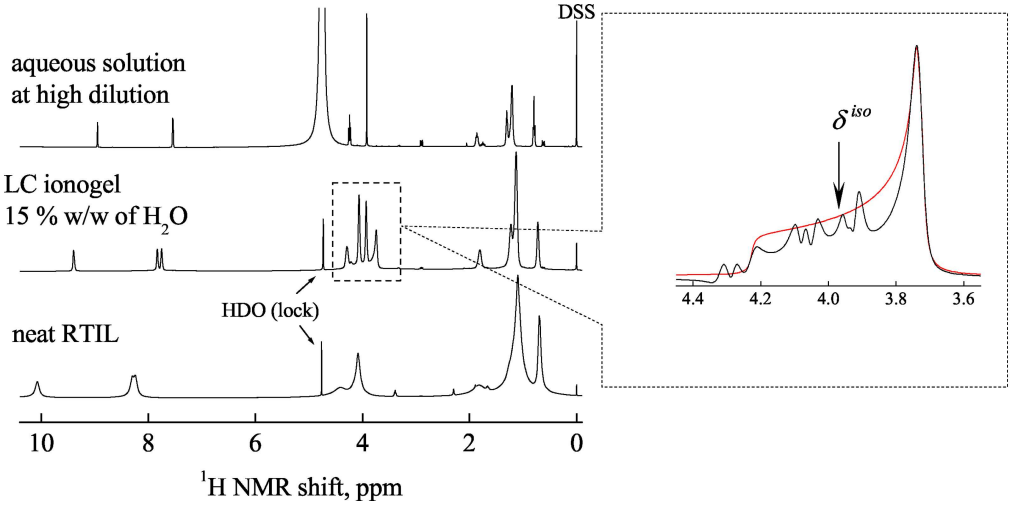

Fig. 5. ^{1}H NMR of spectra of neat [C_{10}mim][Br], in LC ionogel phase and at high dilution in water at room temperature. The fitted anisotropic signal shape after removing H6 and H7 signals is shown in zoom sector. The CSA fitting parameter values are: $\delta^{\text{aniso}} = 0.33$ ppm, $\eta = 0.06$, $\delta^{\text{iso}} = 3.89$ ppm.

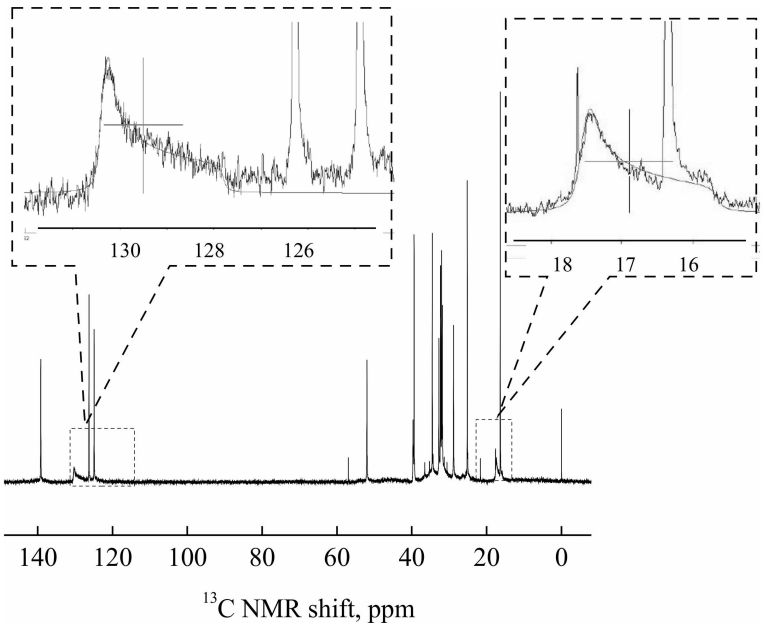

Fig. 6. ^{13}C NMR of spectra of [C_{10}mim][Br] in LC ionogel phase (15% w/w of H_2O) at room temperature. The fitted anisotropic signal shapes are shown in zoom sectors. The CSA fitting parameter values for two processed contours are: $\delta^{\text{aniso}} = -1.69$ ppm, $\eta = 0.11$, $\delta^{\text{iso}} = 129.49$ ppm and $\delta^{\text{aniso}} = -1.25$ ppm, $\eta = 0.12$, $\delta^{\text{iso}} = 16.89$ ppm, respectively.

processed using the chemical shift anisotropy (CSA) shape fitting [28]. The fitted parameter values have been found: $\delta^{\text{aniso}} = 0.33$ ppm, $\eta = 0.06$, $\delta^{\text{iso}} = 3.89$ ppm for ^{1}H (Fig. 5), and for two processed ^{13}C NMR contours $\delta^{\text{aniso}} = -1.69$ ppm, $\eta = 0.11$, $\delta^{\text{iso}} = 129.49$ ppm and $\delta^{\text{aniso}} = -1.25$ ppm, $\eta = 0.12$, $\delta^{\text{iso}} = 16.89$ ppm (Fig. 6), respectively.

In order to obtain additional insight into these experimental observations, the quantum chemistry DFT calculations of ^{1}H and ^{13}C magnetic shielding tensors of [C_{10}mim][Br] and various H_2O structures ($(H_2O)_n$, with $n = 1, \ldots, 5$, i. e. from monomer to H-bonded pentamer) were performed. The results are shown in Figs. 7 and 8.

First of all it becomes obvious why the anisotropic shaped signal was observed in ^{1}H NMR spectra at the position of 3.89 ppm only. According to the experimental CSA fitted and DFT calculated δ^{iso} values (Figs. 5 and 7), the signal at this position can be undoubtedly attributed to the water protons in H-bonded structures.

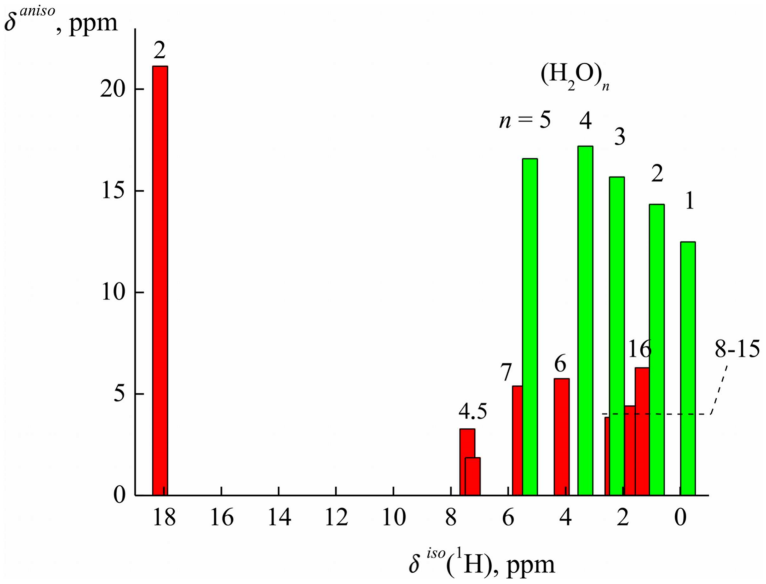

Fig. 7. Calculated ^{1}H chemical shift anisotropy δ^{aniso} versus isotropic chemical shift δ^{iso} for various sites in [C_{10}mim][Br] and H_2O structures ($(H_2O)_n$, with $n = 1, \ldots, 5$); for the site numbering see Fig. 1.

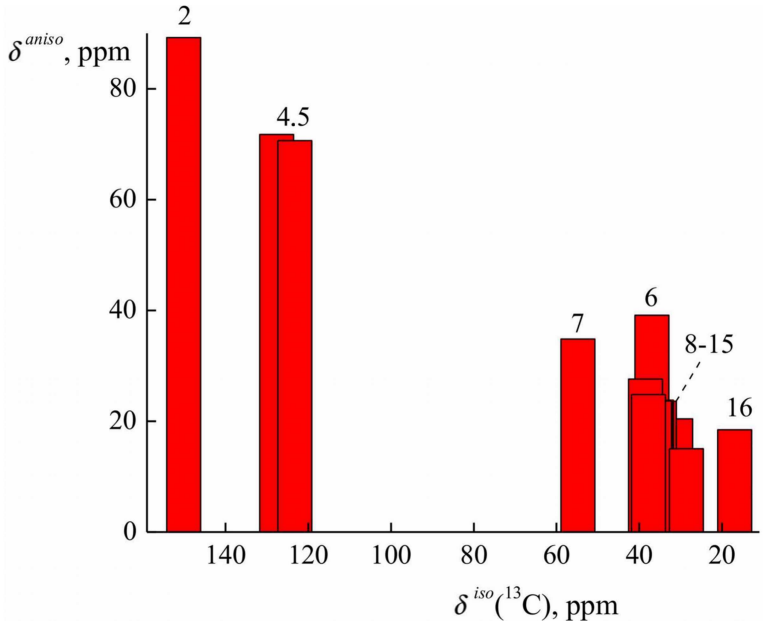

Fig. 8. Calculated ^{13}C chemical shift anisotropy δ^{aniso} versus isotropic chemical shift δ^{iso} for various sites in [C_{10}mim][Br]; for the site numbering see Fig. 1.

The values of chemical shift anisotropies δ^{aniso} for these structures are much higher than those for various protons in [C_{10}mim][Br], except H2 (Fig. 7). However, its anisotropy is very significantly affected (averaged) by H-bond dynamics in $^+$C2–H. . .Br$^-$ bridge (Fig. 1) and thus not pronounced in ^{1}H NMR spectra. For the same reason, also CSA of C2 carbon has not been revealed in ^{13}C NMR spectra. The calculated values of biaxiality (1) for water structures were found to be close to the fitted value ($\eta \approx 0.06$). However, the calculated values of chemical shift anisotropies δ^{aniso} for ^{1}H as well as for ^{13}C are much higher than those observed experimentally. As mentioned above, the applied DFT level was checked in many cases [12–14] and found to be quite adequate for magnetic shielding calculations. Hence such discrepancies between measured and calculated values of chemical shift anisotropies cannot be attributed to the level of theory. It can be supposed that this discrepancy is due to the molecular ordering effects in the lyotropic LC phase [27].

Following this idea, any second-rank tensor that represents a certain *macroscopic* (i. e. experimentally measurable) feature of partially ordered system due to the statistical averaging is related to the *microscopic* (individual, defined by molecular or aggregate structure) tensor via a set of so-called order parameters ($\boldsymbol{S}$). In the present treatment it would mean that the experimentally measured and calculated δ^{aniso} are related as

$$(\delta^{\text{aniso}})_{\text{exp}} \approx |S|\,(\delta^{\text{aniso}})_{\text{calc}}\,, \qquad (2)$$

where $|S|$ is the 'magnitude' of the order parameter. This is only a very rough approach, because the precise expressions of S contain a complex averaging of angular dependences of the orientations of molecular and tensor principal axes frames [27]. It is also known that the values of order parameters for many lyotropic LC and micellar phases are spread ∼0.01–0.2 depending on the site [27]. This allows to explain the significant (∼two orders) discrepancies between measured and calculated CSA values. Also note that the magnitudes of S, evaluated from ^{1}H as well as from ^{13}CNMR data, have very close values, i. e.,

$$\left|\frac{\delta^{\text{aniso}}(^1\text{H})_{\text{exp}}}{\delta^{\text{aniso}}(^1\text{H})_{\text{calc}}}\right| \approx \left|\frac{\delta^{\text{aniso}}(^{13}\text{C})_{\text{exp}}}{\delta^{\text{aniso}}(^{13}\text{C})_{\text{calc}}}\right| \approx |S|\,. \qquad (3)$$

It reveals the difference of lyotropic LC gel phase from the solid one, where the motions of RTIL and water molecules were found from ^{1}H NMR spectra to be dynamically rather segregated (Fig. 3 and the comments above). However, the observed anisotropic ^{13}C NMR signal shape at 16.89 ppm (Fig. 6) points to the difference between LC ionogel and the lamellar phases, where usually a decreasing order parameter moving along hydrocarbon chain from the polar head is observed [27]. It means that the terminal $-CH_3$ groups are more ordered. Hence, the supramolecular structures of [C_{10}mim][Br], similar to some higher micellar RTIL aggregates [23], are expected in the present case.

5. Conclusions

1. The analysis of the composition and temperature effects on ^{1}H and ^{13}C NMR spectra of RTIL provides new valuable information concerning the phase transition molecular motion and ordering in lyotropic liquid-crystalline ionogels.
2. The difference between lyotropic liquid-crystalline (LC) ionogel phase and the solid one has been revealed, the motion of RTIL and water molecules in the latter was found to be dynamically segregated.
3. The observed anisotropic ^{13}C NMR signal shape for the terminal $-CH_3$ group points to the difference between LC ionogel and the lamellar phases, where usually a decreasing order parameter moving along hydrocarbon chain from the polar head is observed. The supramolecular structures of [C_{10}mim][Br], similar to some higher micellar RTIL aggregates are expected.

Acknowledgements

The Danish Center for Scientific Computing (Copenhagen, Denmark) is acknowledged for the possibility to use computational facilities and Gaussian 03 program package. We thank the Institute of Bioorganic Chemistry of Polish Academy of Sciences (Poznan, Poland) for hospitality and NMR facilities. Our special thanks to Prof. Zofia Gdaniec and Dr. Kęstutis Aidas for the assistance.

References

[1] D. Bankmann and R. Giernoth, Progr. Nucl. Magn. Res. Spectrosc. **51**, 63–90 (2007), http://dx.doi.org/10.1016/j.pnmrs.2007.02.007

[2] M.A. Firestone, P. Thiyagarajan, D.M. Tiede, Langmuir **14**, 4688–4698 (1998), http://dx.doi.org/10.1021/la9805995

[3] M.A. Firestone, J.A. Dzelawa, P. Zapol, L.A. Curtiss, S. Seifert, and M.L. Dietz, Langmuir **18**, 7258–7260 2002), http://dx.doi.org/10.1021/la0259499

[4] T. Inoue, B. Dong, and L.Q. Zheng, J. Colloid Interface Sci. **307**, 578–581 (2007), http://dx.doi.org/10.1016/j.jcis.2006.12.063

[5] Y. Gao, L. Hilfert, A. Voigt, and K. Sundmacher, J. Phys. Chem. B **112**, 3711–3719 (2008), http://dx.doi.org/10.1021/jp711033w

[6] T. Fukushima and T. Aida, Chem. Eur. J. **13**, 5048–5058 (2007), http://dx.doi.org/10.1002/chem.200700554

[7] R.T. Kachoosangi, M.M. Musameh, I. Abu-Yousef, J.M. Yousef, S.M. Kanan, L. Xiao, S.G. Davies, A. Russell, and R.G. Compton, Anal. Chem. **81**, 435–442 (2009), http://dx.doi.org/10.1021/ac801853r

[8] J.F. Wishart and E.W. Castner Jr., J. Phys. Chem. B **111**, 4639–4640 (2007), http://dx.doi.org/10.1021/jp072262u

[9] M. Koel, W. Linert, and P. Gärtner, Monatsh. Chem. **138**, V–VI (2007), http://dx.doi.org/10.1007/s00706-007-0790-3

[10] W.M. Gelbart and A. Ben-Shaul, J. Phys. Chem. **100**, 13169–13189 (1996), http://dx.doi.org/10.1021/jp9606570
[11] *Almanac* (Bruker-Biospin, 2011) p. 22
[12] V. Balevicius, Z. Gdaniec, and K. Aidas, Phys. Chem. Chem. Phys. **11**, 8592–8600 (2009), http://dx.doi.org/10.1039/B819666D
[13] V. Balevicius, V.J. Balevicius, K. Aidas, and H. Fuess, J. Phys. Chem. B **111**, 2523–2532 (2007), http://dx.doi.org/10.1021/jp065477x
[14] K. Aidas and V. Balevicius, J. Mol. Liquids **127**, 134–138 (2006), http://dx.doi.org/10.1016/j.molliq.2006.03.036
[15] Gaussian 03, Revision B.05, M.J. Frisch, G.W. Trucks, H.B. Schlegel, G.E. Scuseria, M.A. Robb, J.R. Cheeseman, J.A. Montgomery, Jr., T. Vreven, K.N. Kudin, J.C. Burant, J.M. Millam, S.S. Iyengar, J. Tomasi, V. Barone, B. Mennucci, M. Cossi, G. Scalmani, N. Rega, G.A. Petersson, H. Nakatsuji, M. Hada, M. Ehara, K. Toyota, R. Fukuda, J. Hasegawa, M. Ishida, T. Nakajima, Y. Honda, O. Kitao, H. Nakai, M. Klene, X. Li, J.E. Knox, H.P. Hratchian, J.B. Cross, C. Adamo, J. Jaramillo, R. Gomperts, R.E. Stratmann, O. Yazyev, A.J. Austin, R. Cammi, C. Pomelli, J.W. Ochterski, P.Y. Ayala, K. Morokuma, G.A. Voth, P. Salvador, J.J. Dannenberg, V.G. Zakrzewski, S. Dapprich, A.D. Daniels, M. C. Strain, O. Farkas, D.K. Malick, A.D. Rabuck, K. Raghavachari, J.B. Foresman, J.V. Ortiz, Q. Cui, A.G. Baboul, S. Clifford, J. Cioslowski, B.B. Stefanov, G. Liu, A. Liashenko, P. Piskorz, I. Komaromi, R.L. Martin, D.J. Fox, T. Keith, M.A. Al-Laham, C.Y. Peng, A. Nanayakkara, M. Challacombe, P.M.W. Gill, B. Johnson, W. Chen, M.W. Wong, C. Gonzalez, and J.A. Pople (Gaussian, Inc., Pittsburgh PA, 2003)
[16] J.F. Hinton and K. Wolinski, in: *Theoretical Treatments of Hydrogen Bonding*, ed. D. Hadži (John Wiley & Sons, Chichester, 1997) p. 75
[17] K. Aidas, A. Maršalka, Z. Gdaniec, and V. Balevičius, Lith. J. Phys. **47**, 443–449 (2007), http://dx.doi.org/10.3952/lithjphys.47421
[18] M.H. Levitt, *Spin Dynamics: Basics of Nuclear Magnetic Resonance* (Wiley, Chichester, 2008) p. 205
[19] C.J. Bowlas, D.W. Bruce, and K.R. Seddon, Chem. Commun. 1625–1626 (1996), http://dx.doi.org/10.1039/CC9960001625
[20] V. Balevicius, Z. Gdaniec, K. Aidas, and J. Tamuliene, J. Phys. Chem. A **114**, 5365–5371 (2010), http://dx.doi.org/10.1021/jp909293b
[21] V. Aleksa, J. Kausteklis, V. Klimavicius, Z. Gdaniec, and V. Balevicius, J. Mol. Struct. **993**, 91–96 (2011), http://dx.doi.org/10.1016/j.molstruc.2010.12.060
[22] V. Balevicius, Z. Gdaniec, V. Klimavicius, A. Marsalka, and J. Plavec, Chem. Phys. Lett. **503**, 235–238 (2011), http://dx.doi.org/10.1016/j.cplett.2011.01.035
[23] T. Singh and A. Kumar, J. Phys. Chem. B **111**, 7843–7851 (2007), http://dx.doi.org/10.1021/jp0726889
[24] A. Getsis and A.V. Mudring, Cryst. Res. Technol. **43**, 1187–1196 (2008), http://dx.doi.org/10.1002/crat.200800345
[25] V. Balevičius, Z. Gdaniec, L. Džiaugys, F. Kuliešius, and A. Maršalka, Acta Chim. Slov. (2011) [in press]
[26] Y. Gao, L. Zhang, Y. Wang, and H. Li, J. Phys. Chem. B **114**, 2828–2833 (2010), http://dx.doi.org/10.1021/jp910528m
[27] J. Charvolin and Y. Hendrikx, in: *Nuclear Magnetic Resonance of Liquid Crystals*, ed. J.W. Emsley (D. Reidel Publishing Company, Dordrecht, 1985) p. 449–471
[28] http://anorganik.uni-tuebingen.de/klaus/nmr/index.php?p=conventions/csa/csa

JONINIŲ SKYSČIŲ, FORMUOJANČIŲ LIOTROPINIUS SKYSTAKRISTALINIUS JONOGELIUS, FAZINIŲ VIRSMŲ IR MOLEKULINIŲ JUDESIŲ TYRIMAS ^{1}H IR ^{13}C BMR SPEKTROMETRIJOS METODU

V. Balevičius, L. Džiaugys, F. Kuliešius, A. Maršalka

Vilniaus universieto Fizikos fakultetas, Vilnius, Lietuva

Santrauka

Labai dažnai geliai ir jonogeliai, veikiant įvairiems išoriniams trikdžiams, elgiasi kaip išmaniosios medžiagos. Liotropiniai skystakristaliniai jonogeliai gali susiformuoti tam tikromis sąlygomis maišant joninius skysčius su vandeniu. Eksperimentiškai ištirti vieno iš joninio skysčio – 1-decil-3-metil-imidazolio bromido ([C_{10}mim][Br]) vandens tirpalų – ^{1}H ir ^{13}C BMR spektrai kintant kompozicijai ir temperatūrai. Aptiktas naujas ^{1}H BMR signalas, kuris priskirtas vandens molekulėms. Buvo nustatyta jo anizotropija (0,33 m. d.) ir nulinė asimetrija. Pastebėta kai kurių [C_{10}mim][Br] ^{13}C BMR signalų anizotropija yra 1,2–1,7 m. d. srityje. Atskleisti molekulinių judesių tirpalo kietojoje ir jonogelio fazėse skirtumai. Kietojoje fazėje joninio skysčio ir vandens molekulių dinamika vyksta labai skirtingose laiko skalėse, ir H_2O molekulių dinamika yra ženkliai spartesnė. Jonogelio fazėje jo sandų judesių sparta yra panaši. Kaip parodė kvantinės chemijos skaičiavimai, stebėtąją vandens signalo anizotropiją lemia didelė neasocijuotų H_2O molekulių ir jų H ryšio spiečių protonų magnetinio ekranavimo tenzorių anizotropija, lyginant su joninio skysčio protonais. Ženkli galinės joninio skysčio $-CH_3$ grupės ^{13}C BMR signalo anizotropija išryškina jonogelio ir lamelarinės fazių skirtumus. Pastarojoje dažniausia aptinkamas tvarkos parametro mažėjimas, judant nuo polinio fragmento link uodegos . Tuo tarpu stebimas didesnis galinės $-CH_3$ grupės susitvarkymas jonogelyje byloja, kad šioje fazėje supramolekuliniai dariniai savo struktūra yra artimesni joninių skysčių micelėms.